CHIMIA 42 (1988) Nr. 1 (Januar)

Iron Hydrolysis and the Biochemistry of Iron – The Interplay of Hydroxide and Biogenic Ligands

Walter Schneider: Born 1928 in Adliswil, Kanton Zürich. Dr. phil. II at the Universität Zürich 1955 with Gerold Schwarzenbach. Habilitation at the ETH Zürich 1963. Associate Professor of Inorganic Chemistry, ETH Zürich 1964. Visiting Professor at Illinois Institute of Technology, Chicago 1966/67. Author of «Einführung in die Koordinationschemie», Springer 1968. Full Professor ETHZ 1969. Research on iron hydrolysis aims at applying the results from multi-method studies on isolated systems to the analysis of phenomena occurring in natural waters and living organisms.

Walter Schneider*

The variety of iron hydroxides that are formed in biological systems is considered in terms of prototype products which have been identified in synthetic media. Polynuclear hydroxy-oxo complexes with highly ordered domains are typically obtained in rather acid solutions of ferric ions whereas from strongly alkaline polyalcohol solutions very small polynuclear entities can be isolated. In synthetic solutions, it is practically impossible to prepare iron hydroxides from mononuclear ferric ions. In mammals, however, transferrin releases mononuclear ferric iron into cells. The storage protein, ferritin, is shown to be very selective with regard to the transient species admitted for iron hydroxide deposition. On the other hand, mitochondria are non-selective and use all iron hydroxide complexes for heme synthesis regardless of their nuclearity. Although remote from direct experimental verification, realistic transient iron species can be postulated using the results of studies in synthetic media. Cellular miniaturization via localized iron hydroxide formation in a protein cage is absolutely essential to the kinetic regulation of the iron levels in cells.

1. The Ubiquitous Phenomenon of Iron Hydrolysis

The phenomenon of hydrolysis refers, by definition, to the behaviour of metal salts when they are dissolved in water. Hydrolysis originates in the loss of protons from aqua-metal ions, and it frequently ends in the precipitation of metal hydroxides or hydrous metal oxides. In the range $5 < pH < 9$ which is pertinent to biological as well as aquatic systems, ferric salts hydrolyze immediately whereas ferrous salts are sources of ferrous aqua ions $[Fe(H_2O)_6]^{2\oplus}$, provided the solution is kept free from molecular oxygen or other oxidants. The hydrated Fe^{III} ion is a real species in natural waters and biological fluids whereas the hydrated Fe^{III} ion is confined to artificial media.

It was shown recently that the hydrolysis products which are found in natural systems can be related to prototypes identified in synthetic media [1]. At moderate temperatures, a variety of sols, gels, amorphous and crystalline precipitates emerges from hydrolysis in synthetic aqueous media [1, 2]. In fact, there is abundant evidence that ambient temperature products are documents of their prehistory.

1.1. Sediments, Natural Waters, and Soils

The principal phases of sedimentary origin are hematite, α-Fe_2O_3, and goethite, α-FeO(OH). Ferrihydrite, $Fe_2O_3 \cdot aq$, lepidocrocite, γ-FeO(OH), and maghemite, γ-Fe_2O_3, are moderately widespread whereas akageneite, β-FeO(OH), is rather rare [3]. In the photic zone of lakes, particulate and colloidal iron(III) oxides/hydroxides are a source of $Fe^{2\oplus}$ through photolysis of inner-sphere complexes of iron(III) with biogenic organic ligands [4]. Since the photic zone is aerobic, however, there is a continuous re-oxidation of iron which produces secondary colloidal iron(III) hydroxides. In the deeper layers of a lake, the settling organic products act as reductants in a variety of processes including (1), where formaldehyde is chosen to represent the reduction capacity of biological debris [5].

$$\frac{1}{4}CH_2O + FeO(OH) + 2H^{\oplus} \rightarrow \frac{1}{4}CO_2 + Fe^{2\oplus} + \frac{7}{4}H_2O \quad (1)$$

Strongly eutrophic lakes have a seasonally or permanently reduced hypolimnion providing rather a high concentration of sulfides. Hence, iron sulfides FeS_x, $1 < x \leq 2$, of which pyrite, FeS_2, is thermodynamically the most stable phase, are formed. The formation of siderite, $FeCO_3$, requires high carbonate but negligible sulfide activity.

The mineralogy of lake sediments reflects the fundamental transformation $FeO(OH) \rightleftarrows Fe^{2\oplus}$ taken in conjunction with interactions with sulfide, phosphate, and silicate [6]. Although the relative mass fractions of water and inorganic components are reversed, the inorganic and organic components of the soils are the same as those in natural waters. Furthermore, in both systems there may be considerable variations in the local oxygen and carbon dioxide concentrations. That's why the same types of reactions involving iron call for attention in both systems. However, the bioavailability of iron to plants and microorganisms is an additional, particularly important aspect of iron speciation in soils.

The least stable but most reactive iron(III) form is ferrihydrite which can be considered as a group name for amorphous phases with rather high specific surface areas of the order of some hundred m^2/g. Details of the pathways by which ferrihydrite transforms into the thermodynamically more stable α-FeO(OH) and α-Fe_2O_3 have been elucidated by groups in Ger-

* *Correspondence:* Prof. Dr. W. Schneider
Laboratorium für Anorganische Chemie
Eidgenössische Technische Hochschule Zürich
ETH-Zentrum, Universitätstrasse 6
CH-8092 Zürich

many, Switzerland, and Australia[7]. *Schwertmann* et al. have also investigated the network of transformations linking a ferrous precursor with γ-FeO(OH), γ-Fe_2O_3, and $FeCO_3$[8].

1.2. The Internal Iron Cycle in Humans

Once an atom of iron enters the body, it is in a virtually closed system where it cycles repeatedly (Fig. 1). A small quantity of iron escapes each day, about 1–2 mg, and an equal quantity is absorbed from food. This requirement is met by our daily intake of 10 to 20 mg iron[9]. Heme iron was found to be the optimum form with regard to bioavailability[10]. However, the world's supply of food iron is predominantly in the form of non-heme iron, and with regard to chemical speciation this means Fe^{III} embedded in a matrix of carbohydrates and proteins. It is better, in this case, to think of dispersed iron hydroxides rather than well-defined mononuclear complexes, because the fraction of matrix sites which could prevent hydrolysis of iron(III) entities is virtually negligible. From the point of view of chemical reactions, the fate of iron in the gastrointestinal tract (GIT) raises similar problems to those of the iron circulation in lakes[11].

The present understanding of iron transfer through the mucosal epithelium to the blood stream was outlined recently by *Forth*[12] who emphasized that the translocation and regulation mechanisms have not been fully elucidated as yet. Therefore, it is not surprising that the discussion about whether oral iron therapy should be based on ferrous or ferric preparations continues[13].

It has been pointed out by hematologists that our knowledge of red cell destruction has been derived almost exclusively from the study of cells with a shortened lifespan compared to the normal 120 days[14]. Red cell destruction by macrophages is not accessible to experimental investigation in the same way as is red cell formation or, in particular, red cell maturation[15]. However, it is known that the spleen and the liver are actively involved in red cell destruction, and that the major parts of the body iron stores are located in cells of the liver and the spleen[16, 17].

The storage protein, ferritin[18–20] consists of an iron(III) hydroxide core encapsulated by a protein shell composed, as a rule, of 24 subunits. Core diameters are in the range from 70 to 90 Å and contain some 1000 to 2000 iron atoms; the maximum capacity is about 4500 atoms. This mineral core is reminiscent of particles in lakes. Such a comparison is incorrect, however, because it neglects the role of the protein shell which defines the core size. Why the iron deposition in ferritin cannot be compared with the growth of crystalline FeO(OH) occurring in soil and sediments, is discussed in Section 3.

When the protein shell is removed, the mineral cores assemble to form particulate precipitates. The excessive deposition of the particulate iron hydroxide, hemosiderin, indicates severe perturbation of iron homeostasis[21, 22]. Transfusional overload of thalassemia patients is the most severe disorder of this type[23]. In the healthy state, the deposition in ferritin is balanced by the dissolution of iron hydroxide, which occurs when the stores are mobilized.

The free energy changes related to the iron cycle in Fig. 1 are indicated in Fig. 2.

Thermodynamically, in a neutral aqueous solution, pH 7, and in an atmosphere of oxygen, the ferrous porphyrin is highly unstable with respect to α-FeO(OH). The readily formed ferric porphyrin is perfectly stable with respect to FeO(OH). It is of interest that oxygen itself prevents a mechanistic route of hydrolysis in hemoglobin because the ferrous porphyrin oxidizes at a fast rate only if it is exposed to an aqueous environment. This stability, of course, is lost when the macrocycle is broken up. In the neutral range, a hydrogen atmosphere would be required to destabilize the ferric forms of iron porphyrins, oxides, or transferrins. Actually, this limit of lower potential $E_h \approx -0.5$ V is also effective at the sedimentary interface of eutrophic lakes when CH_4 and H_2S are formed from organic material in conjunction with microbial activity. It is worth remembering that the most reducing iron-sulfur protein couples[27] have redox potentials in this low range, and that they are part of the respiratory chain enzyme systems.

It is explained in Section 3 why iron hydrolysis in cells is confined to compartments with $E_h > +0.2$ V. In the blood stream hydrolysis is prevented thermodynamically by complex formation with chelating cavities in transferrin. We are interested here primarily in the function of transferrins as iron carriers which deliver iron to cells[26, 28]. The stability of the ferric cavity complex breaks down when a car-

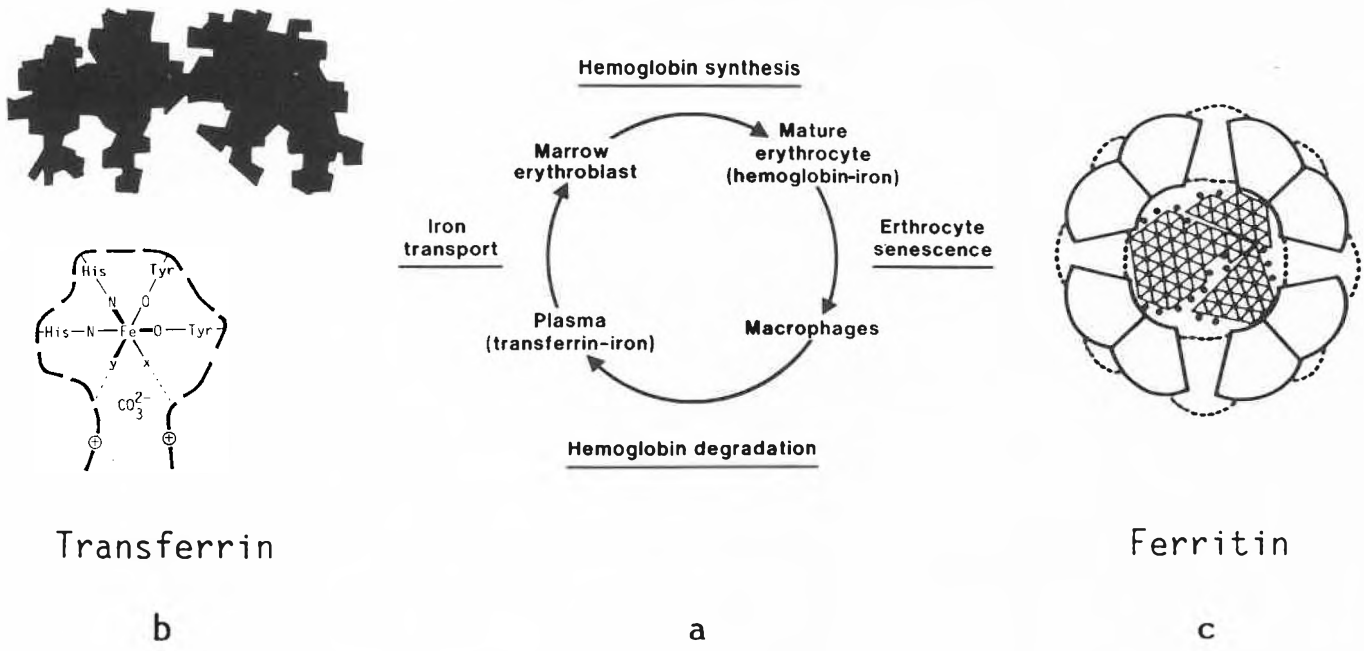

Fig. 1. Internal iron cycle: a) The scheme is copied from Ref.[9]*. Plasma iron derived by the action of the monocyte/macrophage system is bound to transferrin (b) and is ultimately redistributed. The remainder of the iron derived from hemoglobin degradation enters the storage pool as ferritin (c). – b) Transferrin, the carrier protein for metabolic iron. The sketch represents the morphology of the protein according to low-resolution X-ray diffraction data*[26]*. The exact positions of the Fe^{III} sites are not yet known. The model of the Fe^{III} site is based on the experimental evidence available to date. – c) Schematic representation of ferritin indicating the subunit structure of the protein shell (diameter about 120 Å) and the encapsulated iron hydroxide core*[18].

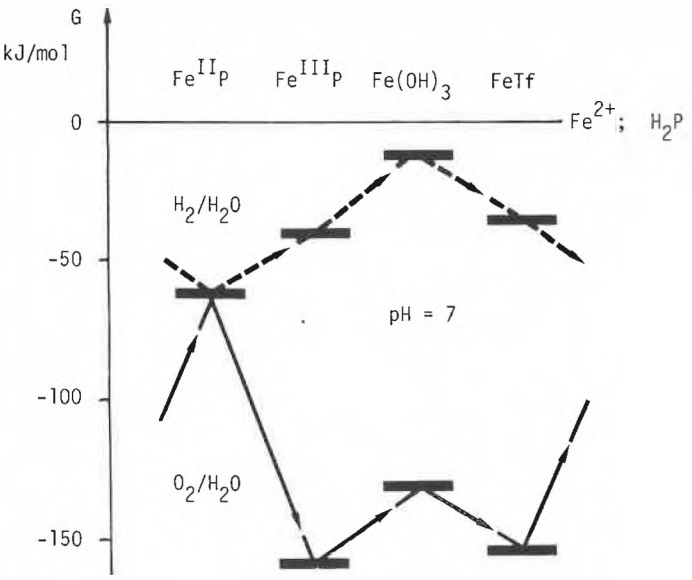

Fig. 2. Free energy profile of the reaction series (2) *to* (5) *involving iron complexes which correspond to those appearing in the internal iron cycle (Fig. 1).*

$$Fe^{2\oplus} + H_2P \rightarrow Fe^{II}P + 2H^{\oplus} \qquad K^* \qquad (2)$$

$$Fe^{II}P + \tfrac{1}{4}\,O_2 + H^{\oplus} \rightarrow Fe^{III}P + \tfrac{1}{2}\,H_2O \qquad E^0(II,III) \qquad (3)$$

$$Fe^{III}P + 2\,H_2O \rightarrow FeO(OH) + H_2P + H^{\oplus} \qquad K_{SO} \qquad (4)$$

$$FeO(OH) + Tf + 3H^{\oplus} \rightarrow Fe^{III}Tf + 2\,H_2O \qquad K' \qquad (5)$$

Equilibrium data were taken from Ref. [24–26] *for porphyrin complexes, FeO(OH), and FeTf (Tf = transferrin). H_2P refers to tetra(N-methylpyridyl)porphyrin. $lgK^* = -1$; $E^0(II,III) = +0.18$ V; $lg\,K_{so} = -39$, $lg\,K' = 20$ (pH = 7).*

bonate ion located in the cavity area is removed. This removal induces the fast expulsion of a Fe^{III} ion.

It is seen in Fig. 2 that the non-physiological reaction (6) should be highly endergonic.

$$Fe^{III}Tf + H_2P + \frac{1}{2}\,H_2O \rightarrow Fe^{II}P + Tf + \frac{1}{4}\,O_2 + 3H^{\oplus} \qquad (6)$$

Alternatively, the non-physiological reaction (7) represents the highly endergonic component of the top cycle in Fig. 2.

$$Fe^{II}P + 2\,H_2O \rightarrow FeO(OH) + H_2P + \frac{1}{2}\,H_2 \qquad (7)$$

In vivo, the intracellular ferritin iron hydroxide is reduced in conjunction with the mitochondrial heme synthesis discussed in Section 3.6.

2. Iron Hydrolysis: The Hierarchy of Factors Determining the Variety of Products

We use the term «iron hydroxide» for any hydrolysis product emerging from hydrolysis in aqueous solution at moderate temperature. «Iron hydroxides» may differ widely with regard to chemical composition, structure, particle size, shape of particles, and interfacial properties[2].

We focus attention on products that are formed from mononuclear iron(II,III) sources. The prime variable which determines the product's properties is the pH and its rate of change as a function of space and time[1,2].

It is useful to describe products and their evolution in terms of polynuclear cores which are defined as containing $OH^{\ominus}$ and $O^{2\ominus}$ exclusively in bridging positions.

$$Fe_pO_r(OH)_s \qquad Fe(OH)_{\bar{n}} \qquad \bar{n} = \frac{2r+s}{p} \qquad (8a)$$

$$Fe_pO_r(OH)_s \cdot (H_2O)_w^z \qquad (8b)$$

$$Fe_pO_r(OH)_s \cdot (L)_i^{z'} \qquad (8c)$$

It is rather exceptional to find a precipitate containing cores that have the same composition (p, r, s) within narrow limits. *Schwyn*[1] determined the size and shape of polynuclears in homogeneous chloride solution by laser light scattering methods, and he identified monodisperse systems with p up to 60000 while $\bar{n} = 2.7$ was constant over the whole range of p. In this system, hydrolysis was induced from the low pH region.

Peripheral iron(III) sites of polynuclears imply local units $FeO_i(OH)_j$ with $i + j \leq 5$. Hence, there is at least one H_2O molecule coordinated to each interfacial Fe^{III}. These coordinated water molecules, of course, have characteristic pK values for the proton transfer equilibria (9).

$$\gtrless Fe^{III}OH_2^{\oplus} \underset{+\,H^{\oplus}}{\overset{-\,H^{\oplus}}{\rightleftharpoons}} \gtrless Fe^{III}OH \underset{+\,H^{\oplus}}{\overset{-\,H^{\oplus}}{\rightleftharpoons}} \gtrless Fe^{III}O^{\ominus} \qquad (9)$$

The charges assigned in Equation (9) are a conventional way of indicating correct relative values. For polynuclears in homogeneous solution, neither the intrinsic nor the average pK values are experimentally accessible. The net charge, defined by the difference between positive and negative sites according to (9) is zero at one singular pH value termed the point of zero charge (PZC). Positively charged polynuclears are polyelectrolytes which specifically adsorb anions to the limit of coagulation. Perchlorate is least effective in this interfacial adsorption, hence it is convenient to study polynuclears of type (8b) in perchlorate media. When the pH is raised, coagulation, induced by the deprotonation of peripheral water molecules, prevents the determination of the PZC.

Schindler and *Stumm*[29] showed that the surface chemistry of solid metal oxides and hydroxides is well understood in terms of the coordination chemistry of surface sites. Intrinsic surface acidity constants are used to describe proton transfer equilibria, and the substitution of water by ligands is handled using intrinsic stability constants.

$$\gtrless Fe{-}OH_2^{\oplus} \rightleftarrows \gtrless Fe{-}OH + H^{\oplus} \qquad p{K}^{s}_{a1} = 6.4 \qquad (10)$$

$$\gtrless Fe{-}OH \rightleftarrows \gtrless Fe{-}O^{\ominus} + H^{\oplus} \qquad p{K}^{s}_{a2} = 9.3 \qquad (11)$$

$$\gtrless Fe{-}OH + H_2PO_4^{\ominus} \rightleftarrows \gtrless FeHPO_4^{\ominus} + H_2O \qquad lg\,K^{s}_{int} = 7.0 \qquad (12)$$

The data in Equations (10)–(12) indicate a PZC of roughly 8 for α-FeO(OH). Phosphate forms quite strong surface complexes involving $HPO_4^{\ominus}$ [30]. Actually, the tendency to form surface complexes with acetate, oxalate, salicylate, catecholate, and similar ligands can be correlated with the stability of mononuclear complexes in homogeneous solution[29,30].

As a rule, the equilibria of type (13) are shifted far to the left at around pH = 7 ± 1.

$$FeO(OH) + 3\,HL \rightleftarrows FeL_3 + 2H_2O \qquad (13)$$

This is particularly true for carboxylic acids, amino acids, and oligopeptides[31].

Prominent exceptions are acethydroxamic acid, tiron (4,5-dihydroxybenzene-1,3-disulfonic acid), and ethylenediaminetetraacetic acid (EDTA); all three compounds contain structural units which are found in the siderophores that microbes synthesize for iron acquisition[32]. The surface complexes with ligands of this type are kinetically important intermediates in the dissolution reaction. It is quite clear that polynuclears of type (8c) and with rather low p can have appreciable lifetimes only if the acid HL is unable to dissolve iron hydroxides.

In view of our need to understand the structure of ferritin mineral cores and the pathways of their formation it is important to assess the varieties of polynuclears (8b, c) which are accessible to experimental studies.

2.1 Iron Cores with Low Nuclearity

The data of *Schindler*[33,34] were very important in showing that the dinuclear complex $[Fe_2(OH)_2]^{4\oplus}$ is thermodynamically unstable with respect to the mononuclear $Fe^{3\oplus}$ and the solid phase FeO(OH) in perchlorate solution.

$$[Fe_2(OH)_2]^{4\oplus} \rightarrow H^{\oplus} + Fe^{3\oplus} + \alpha\text{-FeO(OH)} \quad (14)$$

However, the hydrated dinuclear is kinetically very inert in dilute solutions at pH ≤ 2 when excess $Fe^{3\oplus}$ is present. Under these conditions precipitation times are of the order of months[1,34]; they are rather ill-defined because nucleation is heterogeneous. The barrier to homogeneous nucleation is the activation energy of step (15) and subsequent steps in the growth of polynuclears.

$$[Fe_2(OH)_2]^{4\oplus} + FeOH^{2\oplus} + H_2O \xrightarrow{k_{23}} [Fe_3(OH)_4]^{5\oplus} + H^{\oplus} \quad (15)$$

We estimate

$$\Delta G^{\neq} = \Delta G^{\neq}_{OS} + \Delta G^{\neq}_{PT} \geq 130\ kJ \cdot mol^{-1} \quad (16)$$
$$(80) \quad (50)$$

$$k_{23} \leq 10^{-9}\ M^{-1}\ s^{-1}$$

for the reaction (15). The terms on the right hand side of (16) refer to the endergonic encounter and to the proton transfer from the collision pair to the solvent, respectively.

The growth of polynuclears with a β-FeO(OH) structure was induced when macrocrystals of NaCl were added to oversaturated $[Fe_2(OH)_2]^{4\oplus}$ solutions[1], whereas, in dust-free solutions, the equivalent amount of dissolved NaCl had no effect. When polynuclear growth is induced in acid solution, even the simple ions $Cl^{\ominus}$ and $NO_3^{\ominus}$ exert specific anion effects as indicated by the data in Table 1.

Table 1. Evidence for specific anion effects associated with the hydrolysis of Fe^{III} species in acid solution. Ionic strength I_c(NaX); 25 °C; $f = -1gK_{so}/\bar{n}$.

$X^{\ominus}$	I_c	Precipitate	$\bar{n}$	$-1gK_{so}$	f	Ref.
$ClO_4^{\ominus}$	3	amorphous FeO(OH)	3	39	13	[34]
$Cl^{\ominus}$	0.5	$Fe(OH)_{2.7}Cl_{0.3}$	2.7	35	13	[35]
$NO_3^{\ominus}$	1	$Fe(OH)_2NO_3$	2.0	26	13	[36]

None of the anions in Table 1 form salts which contain the cationic hydrated cores **1**–**3**.

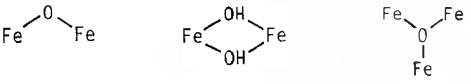

1 **2** **3**

It is easy to understand that **3** is very unstable with respect to the mononuclear species in Equation (17).

$$[Fe_3O]^{7\oplus} + H_2O \rightarrow 2\,[FeOH]^{2\oplus} + Fe^{3\oplus} \quad (17)$$

On the other hand, all these cores appear as structural fragments in a variety of complexes obtained from mononuclear precursors (Table 2).

Table 2. Complexes with the cores **1, 2, 3** formed from mononuclear precursors $[FeL_3(H_2O)]$ or $[FeL_2(OH)(H_2O)]$. phen = 1,10-phenanthroline; Hpic = picolinic acid; TPP = tetraphenylporphyrin; H_2xyl = xylitol.

Core	Complex	Ref.
1	$[(Fe\ EDTA)_2O]^{4\ominus}$	[37]
	$[(Fe\ phen_2)_2O]^{4\oplus}$	[38]
	$[(Fe\ TPP)_2O]$	[39]
2	$[pic_2Fe(OH)]_2$	[37]
	$[xyl_2Fe(OH)]_2^{4\ominus}$	[46]
3	$[Fe_3O(O_2CCH_3)_6]^{\oplus}$	[40]

The hydrolytic disproportionation of complexes $[FeL_n(OH)(H_2O)]$ is quite often exergonic over the range pH = 7 ± 2.

$$3\,[Fe(tir)_2OH]^{6\ominus} \longrightarrow 2\,[Fe(tir)_3]^{9\ominus} + Fe(OH)_3 \quad (18)$$

$$6\,[Fe(nta)OH]^{\ominus} \xrightarrow{3\,H_2O} 3\,[Fe(nta)_2]^{3\ominus} + 3\,Fe(OH)_3 + 3\,H^{\oplus} \quad (19)$$

In such cases the dinuclear species with μ-diol bridges are intermediates in the overall reaction. As a rule, the dinuclears are formed at a fast rate, typical rate constants k_D are in the range 10^2 to $10^3\ M^{-1}s^{-1}$ at room temperature[41].

$$2\{Fe^{III}OH(H_2O)\} \xrightarrow{k_D} \{Fe(OH)_2Fe\} + 2\,H_2O \quad (20)$$

The compatibility, or the symbiosis, of ligands L with $OH^{\ominus}$ or $O^{2\ominus}$ in mononuclear as well as in polynuclear complexes, depends very much on

a) the activity of $OH^{\ominus}$ in the solution;

b) the mole fraction of H_2O which may be kept low in non-aqueous solvents.

In the solvent systems $CH_3CO_2H/CH_3CO_2^{\ominus}$, $Na^{\oplus}/H_2O$, the trinuclear complex **4** with the core **3** prevails at low x_{H_2O} whereas large polynuclears, and finally, hydroxide precipitates are formed when water is added.

$$[Fe_3O(O_2CCH_3)_6(H_2O)_3]^{\oplus}$$
4

In the final product, acetate is just «adsorbed» on the iron(III) hydroxide particles and this means that there are surface complexes $Fe^{III}O_2CCH_3$ which are decomposed when the pH is raised beyond 6.

Recently, *Lippard*[42] isolated polynuclear complexes **3′**, **5′**, **6′** containing the cores **3**, **5**, and **6** from acetonitrile or tetrahydrofuran solutions with low x_{H_2O}. Consequently, these

$Fe_3O^{7\oplus}$ $[Fe_3O(O_2CPh)_2(TIE\text{-}O)_2Cl_3]$

3 **3′**

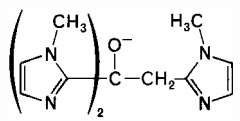

TIE-O⁻

$Fe_4O_2^{8\oplus}$

5

$[Fe_4O_2(O_2CPh)_4(BIC\text{-}O)_2(BIC\text{-}OH)_2]$

5′

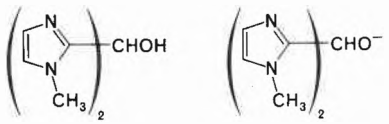

(BIC–OH) (BIC–O⁻)

$Fe_{11}O_6(OH)_6^{15\oplus}$ $[Fe_{11}O_6(OH)_6(O_2CPh)_{15}]$

6 **6′**

products decompose in water at pH > 3 as illustrated by Equation (21) for compound **3′**.

$$[Fe_3O(O_2CPh)_2(TIE\text{-}O)_2Cl_3] + 8\,H_2O \rightarrow 3\,Fe(OH)_3 + 2\,PhCO_2H + 2\,TIE\text{-}OH + 3\,Cl^{\ominus} + 3\,H^{\oplus} \quad (21)$$

In fact, the polynuclears **5′** and **6′** are intermediates in the hydrolysis of $Fe^{3\oplus}$ which had been scavenged by the excess of carboxylate, nitrogen and oxygen ligand groups. In contrast to these complexes

which do not fit into aquatic or biological media, the dinuclear complex **7** is an illuminating model of the iron(III) sites in hemerythrin[43].

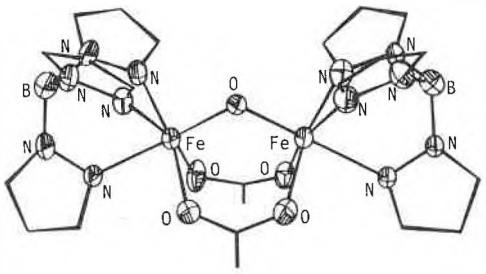

7

The dinuclear **7** is stable around pH 4 in aqueous solution. The self-assembly of this dinuclear shows that the stability of the iron(III) inserted into the protein of hemerythrin is not enforced merely by steric constraints. It is very likely that the protein complex was even more stable than the model complex **7**. At any rate, the structure of type **7** inhibits further hydrolysis for thermodynamic reasons.

2.2 The Growth of Polynuclear Crystallites

Hydrolysis in chloride solution illustrates a case of crystal growth in solution[1,2]. Chloride effects operate at all levels, in nucleation, in growth, and in the ageing processes of polynuclears with β-FeO(OH) structure. The time evolution of the size (p) and the shape was elucidated by a variety of methods and simulated by Monte Carlo procedures[44].

$$p\,Fe^{3\oplus} + 2.7\,OH^{\ominus} \rightarrow |FeO_{2/3}(OH)_{4/3}]_p^{p\oplus/3} + \frac{2}{3}\,p\,H_2O \qquad (22)$$

$$Fe^{III}\ \ 0.05\text{–}0.4\ \text{M} \qquad Cl^{\ominus}\ \ 0.2\ \text{–}1.5\ \text{M} \qquad (23)$$

The stoichiometry (22) was found over the entire range of educt solution compositions (23). The Mössbauer data[45] (Fig. 3) were important in proving that the average local electronic environment of Fe^{III} in the polynuclears persisted a) during progressive base addition and b) upon ageing at constant composition.

Fig. 4 provides a typical record of experimental quantities as a function of time. The pH of the solutions covers the range $1 \leq pH \leq 2.5$ where the predominant mononuclear species are $Fe^{3\oplus}$ and $Fe(OH)^{2\oplus}$ together with weak chloro complexes $FeCl^{2\oplus}$ and $FeCl(OH)^{\oplus}$. The fact that polynuclears with well defined structures are formed indicates the existence of growth processes, which on the level of local surface site reactions involve one predominant reactant, i.e. $Fe(OH)^{2\oplus}$[1].

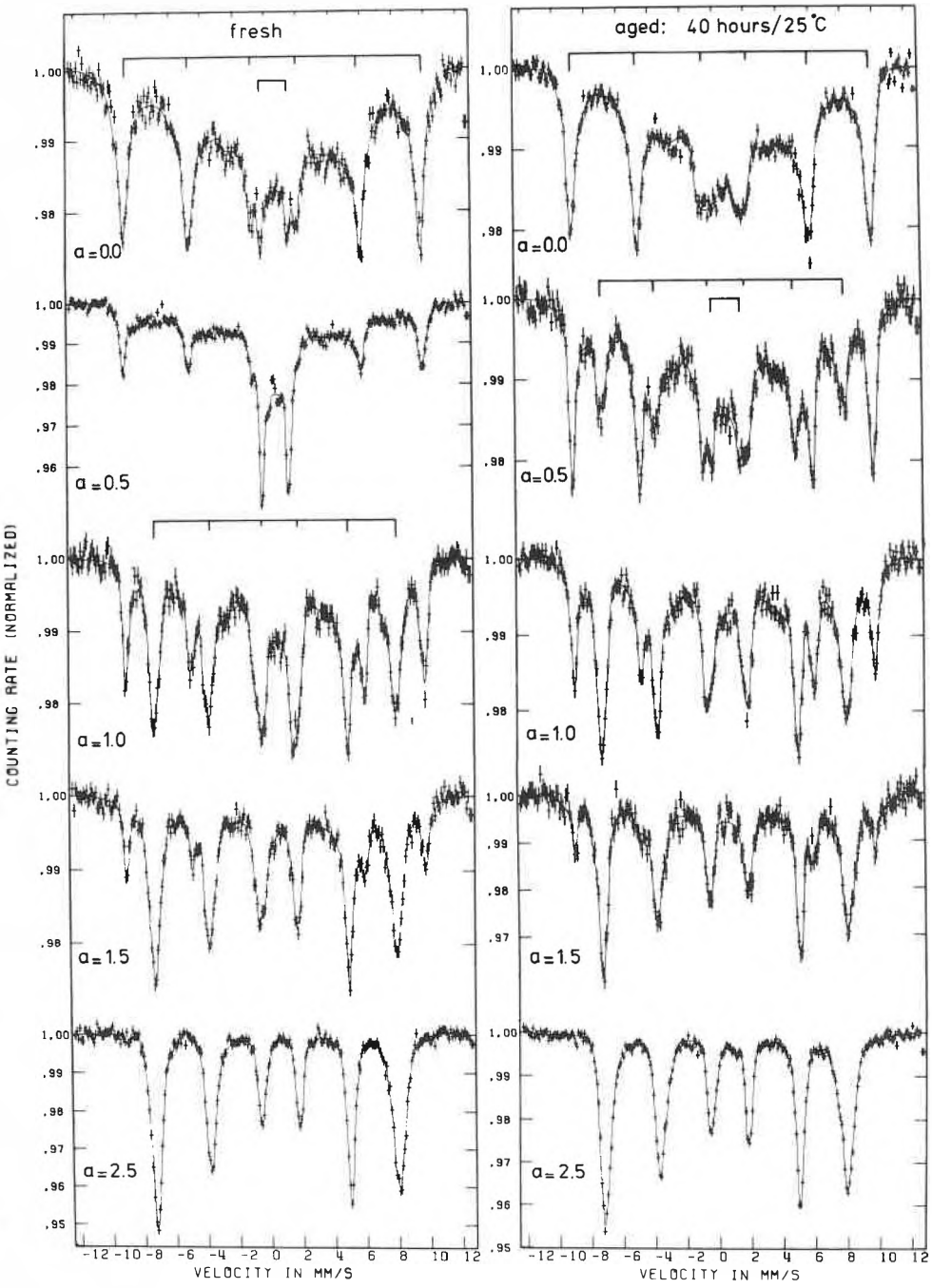

Fig. 3. Mössbauer spectra of frozen solutions of polynuclear species with β-FeO(OH) structure[45]*. The educt solutions had a chloride concentration of 1.5–2.0* M *and various* a *values (*a = *equivalent of base per iron). Fresh samples were prepared within (*a + 1*) hours from strongly acid ferric chloride solutions. The total iron concentration was 0.3–0.5* M*. The spectra were taken at ca. 20 K. The two dominant spectra refer to $Fe^{3\oplus}$, and to polynuclears with the core $[FeO_{2/3}(OH)_{4/3}]_p$, respectively. The spectral parameters are: magnetic hyperfine field H = 580 (470) kOe; quadrupole splitting ε = −0.06 (−0.06) mm/s; isomer shift δ = +0.52 (+0.47) mm/s.*

In the simulation model, relative rate parameters for the addition of one simple iron atom, i.e. individual steps $p \rightarrow p + 1$, and the removal of Fe^{III}, i.e. steps $p \rightarrow p - 1$, were assigned[44]. The structure of the polynuclears as well as rate parameters for well-known substitution reactions were essential features of this assignment. The modelling of the early stages of nucleation covering the range $2 \leq p \leq 9$ required the set of 61 species some of which are shown in Fig. 5. As an example, one of the polynuclears of this set is shown explicitly in Fig. 6.

The same parameters that were successful in reproducing the anisotropic growth of needle-shaped polynuclears were also applied to modelling of the ageing phase. Ageing involves the increase in width and the shrinkage in length of the polynuclears when p remains essentially constant. In Fig. 7 some experimental data are compared with results from the simulation of ageing.

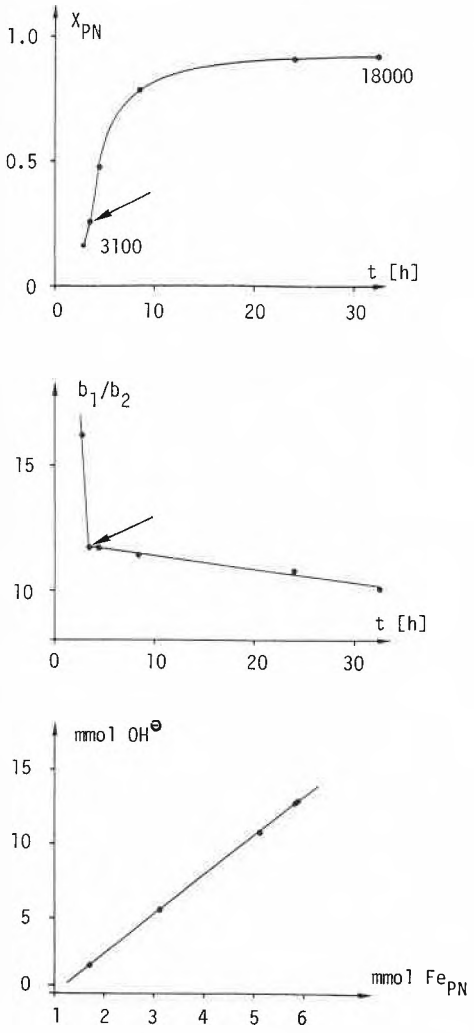

Fig. 4. The growth of polynuclear species with β-FeO(OH) structure in a seeded solution at constant pH = 2 and with Fe^{III} 0.06 M; $Cl^{\ominus}$ 0.2 M; $ClO_4^{\ominus}$ 0.8 M ($Na^{\oplus}$). x_{PN} = polynuclear iron per total iron. – Top: Polynuclear seeds with p = 3100 correspond to x_{PN} = 0.15 when the pH is adjusted. The arrow refers to the transition point indicated in b). – Middle: The ratio of length to width of the polynuclears in a) according to dynamic light scattering data. The arrow indicates the transition from the strongly anisotropic growth in one preferential direction to a growth phase with nearly equivalent growth in length and in width. – Bottom: The molar ratio of base consumed per Fe_{PN} formed in the interval from p = 3100 to p = 18000 (part a); $\bar{n}$ = 2.65.

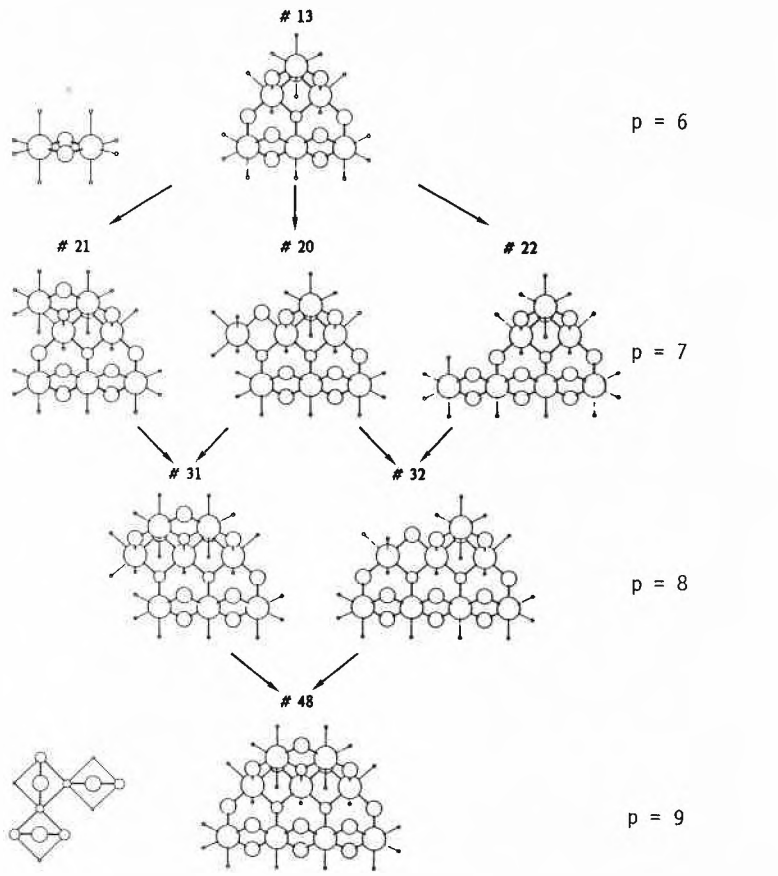

Fig. 5. Some of the 61 polynuclear cores included in the modelling of the early stages of polynuclear growth in the range from p = 2 to p = 9 [44]. Arrows indicate the preferential growth steps from core 13 (p = 6) to core 48 (p = 9) which is built up in preference to 15 other reasonable structures with p = 9. Circle diameters decrease in the series $Fe^{3\oplus} > OH^{\ominus} > O^{2\ominus} > H_2O$.

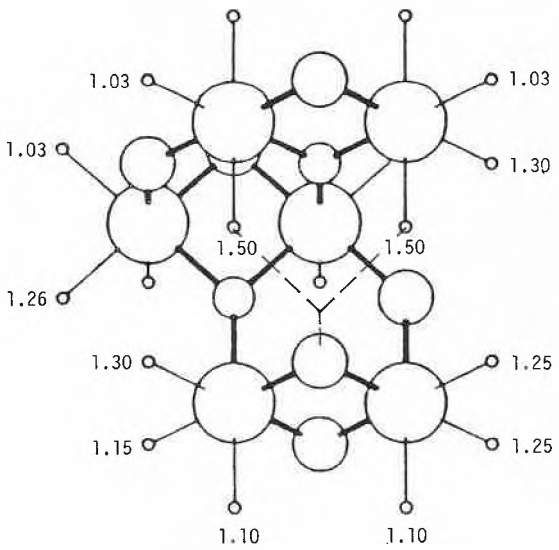

Fig. 6. The idealized structure of the polynuclear core $[Fe_6O_2(OH)_6]^{8\oplus}$. The numbers indicate the (−) potential energy of $Cl^{\ominus}$ in contact with water molecules. They were calculated from point charge models (DK = 1); the unit is 1390 kJ/mol [44]. The regiospecific association of $Cl^{\ominus}$ was an important concept in the modelling of polynuclear growth.

2.3. Gel Formation from Cyclic Polynuclears

The fully deprotonated $[Fe(H_2O)_6]^{3\oplus}$, which means $[Fe(OH)_6]^{3\ominus}$, does not exist in aqueous solution even in strongly alkaline solutions. It would be tempting to follow the formation of $FeO(OH)_{(s)}$ from the alkaline side (24).

$$[Fe(OH)_6]^{3\ominus} + 3\,H^{\oplus} \rightarrow FeO(OH) + 4\,H_2O \quad (24)$$

$$[Fe(sor)_3]^{3\ominus} + 3\,H^{\oplus} \rightarrow FeO(OH) + 3\,H_2sor \quad (25)$$

H_2sor = sorbitol $HOCH_2(CHOH)_4CH_2OH$

In fact, crystalline α-FeO(OH) is obtained when synthetic ferrihydrite is heated at pH ≥ 12 for some hours [7]. It is believed that the crystal growth proceeds via the mononuclear $[Fe(OH)_4]^{\ominus}$.

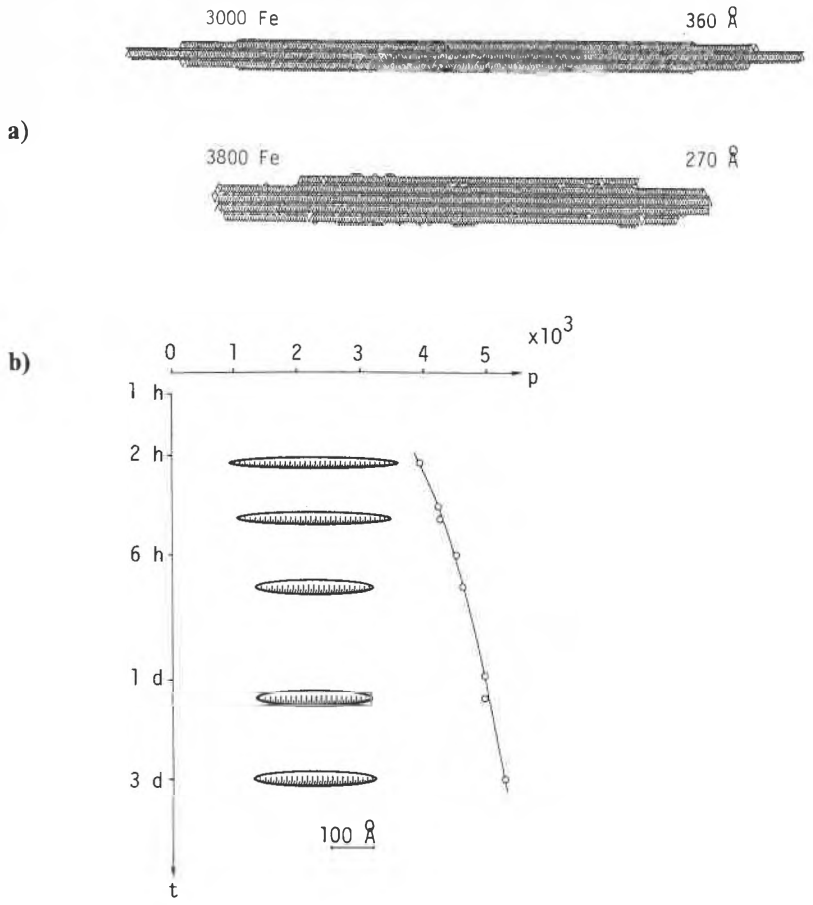

Fig. 7. Ageing of polynuclear species with β-FeO(OH) structure. – a) Modelling of the ageing under near-saturation conditions. The model educt crystallite contains p = 3000 Fe; the ratio of the length to the width is 20. The kinetic parameters were assigned according to the concepts developed in the modelling of the early stages (Fig. 5 and Fig. 6). The product crystallite shown (p = 3800) emerged from 50000 simulation steps involving p → p ± 1 reactions. – b) Experimental data of Schwyn [2] on the ageing of polynuclears with p = 4000. The structure is preserved while the crystallites are shortening and widening. The grating is 6 Å, i.e. twice the height of the tetragonal unit cell of β-FeO(OH).

Mononuclear anionic species $[Fe(sor)_3]^{3\ominus}$ have been identified in strongly alkaline sorbitol solutions [1,46] at pH beyond 14. It is estimated that the conventional stability constant of these trisbidentate complexes is very high (26)

$$[Fe(sor)_3]^{3\ominus} \quad ; \quad \lg \beta_3 \geq 45 \tag{26}$$

whereas the conditional equilibrium constant for (26) indicates complete hydrolytic decomposition to precipitates in the range $5 < pH < 9$.

$$FeO(OH)_{(s)} + H_2O + 3\ H_2sor \overset{K}{\rightleftarrows} [Fe(sor)_3]^{3\ominus} + 3\ H^{\oplus} \tag{27}$$

$$K_{cond} = K \cdot [H^{\oplus}]^{-3} = \frac{[Fe(sor)_3]}{[H_2sor]^3}$$

pH	5	7	9
$-\lg K_{cond}$	21	15	9

It is all the more surprising that, if the pH-gradients are kept low in the neutralization procedure [1,46], homogeneous solutions persist from high pH down to pH = 7. In fairly concentrated solutions with total Fe^{III} larger than 0.1M, transparent gels which do not change over a period of a few months, appear. This gel formation is reversible, which means that the structural unit is preserved when weaker interactions between these units induce gelation.

The experimental data obtained in homogeneous solution add up to the structure assignments in Fig. 8.

It is useful to postulate that the relevant mononuclear species involved in the strikingly simple scheme in Fig. 8 is $[Fe(sor)_2OH]^{2\ominus}$. It is instructive to simulate the evolution of polynuclears according to Fig. 9.

The cyclic polynuclear turns out to be a thermodynamic as well as a kinetic sink when physically meaningful kinetic parameters are assigned [47].

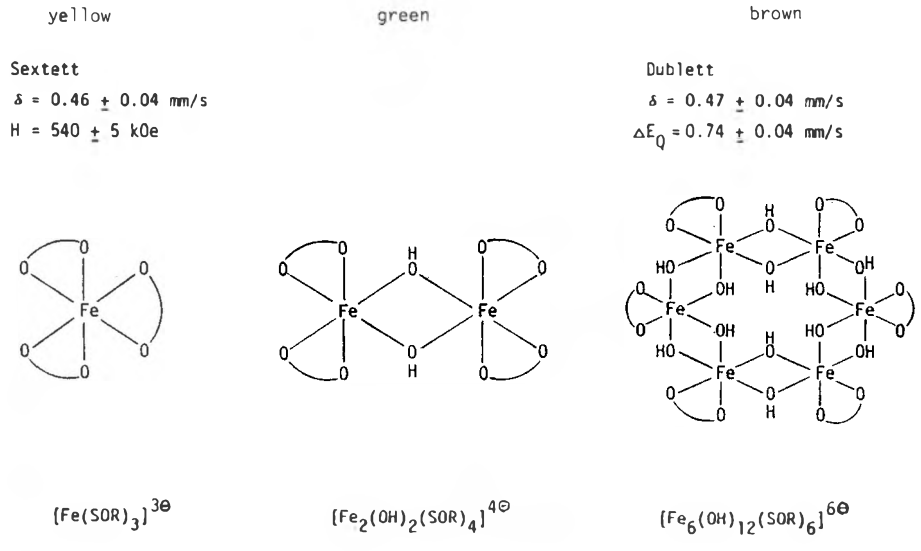

Fig. 8. The structure assigned to iron(III) species in sorbitol solutions. The mononuclear $[Fe(sor)_3]^{3\ominus}$ exists at pH > 14 and is the precursor of the dinuclear, and the hexanuclear obtained by cautious neutralization which, in rather concentrated solutions, leads to gels at pH ≤ 9 [1,46]. δ: isomer shift; E_Q: quadrupole splitting; H: magnetic hyperfine field.

2.4. Realistic and Fictitious Mononuclears

It is useful to consider the series of mononuclears (28).

The data in Table 3 refer to experimental data as well as to estimates discussed in Ref. [1,2] and references therein. There is no doubt that the properties change dramatically from left to right in the series (28).

In the present context, it is particularly important to realize that the water in the first sphere of the aqua-hydroxo complexes $[Fe(OH)_3 \cdot aq]$ and $[Fe(OH)_4 \cdot aq]^{\ominus}$ is so labile as to permit virtually diffusion-controlled rates of water substitution.

In the laboratory we can not prepare solutions of the mononuclear iron hydroxide mn-$Fe(OH)_3$ which, if it did not react with itself, would prevail in biological and aquatic media. The first step (29) is the

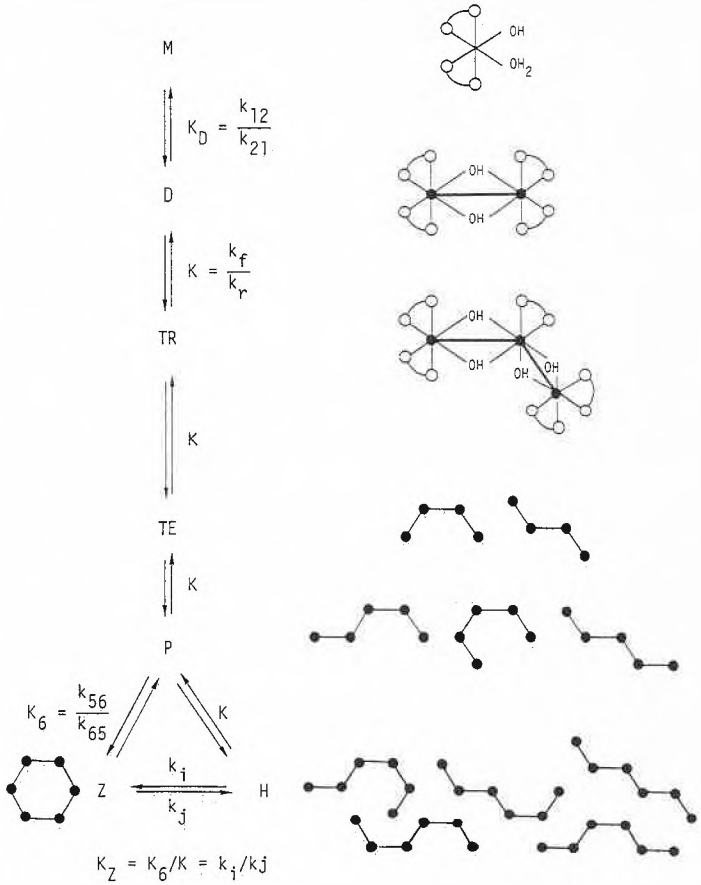

Fig. 9. The hypothetical scheme of reactions leading to the cyclic hexanuclear. The isomerization of open-chain isomers with the same nuclearity p = 4, 5, 6 would proceed at a faster rate than the growth or dissociation in steps p → p ± 1. The cyclic hexanuclear prevails under conditions where [Fe(sor)$_2$OH]$^{2\ominus}$ is stable with respect to [Fe(sor)$_3$]$^{3\ominus}$ and H$_2$sor. This implies that K, $K_D \gg 1$; $k_j \ll k_r \approx k_{21}$; $k_i \gg k_{21}$ and consequently $K_6 \geq 10^{+4}K$.

$$\begin{array}{lccccc} & Fe^{3\oplus} & FeOH^{2\oplus} & Fe(OH)_2^{\oplus} & Fe(OH)_3 & Fe(OH)_4^{\ominus} \\ pK & 3 & 3.3 & \approx 6 & \approx 9 & \end{array} \quad (28)$$

Table 3. Kinetic properties of mononuclear aqua-hydroxo complexes Fe(OH)$_i^{3-i}$aq; 25 °C; k_{ii} refers to the dimerization reaction. Estimated values in the lower part indicate that k_{33} most likely reaches the diffusion controlled limit.

Mononuclear	$\lg k_{ex}^{H_2O}$[s^{-1}]	$\lg k_{ii}$[M^{-1}s^{-1}]
[Fe(H$_2$O)]$^{3\oplus}$	2	–
[Fe(OH)(H$_2$O)$_5$]$^{2\oplus}$	5	3
[Fe(OH)$_2$(H$_2$O)$_4$]$^{\oplus}$	> 7	> 5
[Fe(OH)$_3$·aq]	> 9	> 7

analogous reaction to (20) but the rate constant $k_{33} \geq 10^{+7}$M^{-1}s^{-1} is much larger than k_D.

$$2\ \text{mn-Fe(OH)}_3 \xrightarrow{k_{33}} \{(HO)_2Fe(OH)_2Fe(OH)_2\} \quad (29)$$

At the level of 0.1 mM mn-Fe(OH)$_3$ the half-time of the dimerization would be in the order of milliseconds. That's why products obtained from base addition to acid solutions of hydrated Fe$^{3\oplus}$ reflect the kinetics of the mixing procedure[1,2]. In order to check the rate of reaction (29) experimentally, it was necessary to maintain a controlled supply of mn-Fe(OH)$_3$ to a reactor in which the product formation could be monitored. This is a rather fictitious situation on the macroscopic scale but it is very likely that mn-Fe(OH)$_3$ is a realistic species in cells (Section 3).

2.5. Oxidatively Induced Hydrolysis

In biological fluids, in soils, and in aquatic systems the ferrous ion Fe$^{2\oplus}$ will hardly reach concentrations of 0.01 mM which is a lower limit from the point of view of many laboratory experiments.

At pH 7, the instantaneous oxidation product of hydrated Fe$^{2\oplus}$ is mn-Fe(OH)$_3$. In fact, the oxidation by molecular oxygen would be endergonic with regard to the first three one-electron transfer steps if the instantaneous product were [Fe(H$_2$O)$_6$]$^{3\oplus}$ in each step. It is shown in Fig. 10 that the situation is quite different if proton transfer precedes the electron transfer.

The kinetics of oxygenation[48] indicate that electron transfer occurs in conjunction with proton transfer from hydrated Fe$^{2\oplus}$ to the water medium. This suggests that polynuclear species obtained via oxidation of Fe$^{2\oplus}$ should reflect the characteristic properties of mn-Fe(OH)$_3$, Fe(OH)$_2^{\oplus}$ or Fe(OH)$_4^{\ominus}$ depending on the pH of the solution.

The only way to measure the size of polynuclears, at present, is by laser light scattering methods[49]. Small polynuclears with p in the range 5 to 50 are detectable in solutions where the total iron concentration is at least 0.01 M. On thermodynamic grounds, it seems trivial that the products are precipitates which appear immediately after oxygen consumption. However, the precipitates consist of small, primary polynuclears which coagulate very rapidly. This coagulation can be inhibited by additives which are preferentially adsorbed at the polynuclear/solvent interface. It was found recently that TRIS-buffer components are very effective in scavenging low nuclearity products of oxidatively induced hydrolysis[50]. The data in Fig. 11 show that the particles as seen by the light scattering method are larger than those determining the kinetics of acid decay.

This is the experimental basis for the identification of the aggregate structure of iron(III) hydroxide particles. We use the term «particle» here in a morphological sense. The Fe^{III}-OH$^{\ominus}$/O$^{2\ominus}$ bonding within the polynuclear core is far stronger than the interactions between polynuclears which induce aggregation prior to coagulation.

It is quite clear that there is a wealth of interactions including outer- and inner-sphere phenomena at interfacial Fe^{III} sites, and that these effects are enhanced by increasing surface to volume ratios.

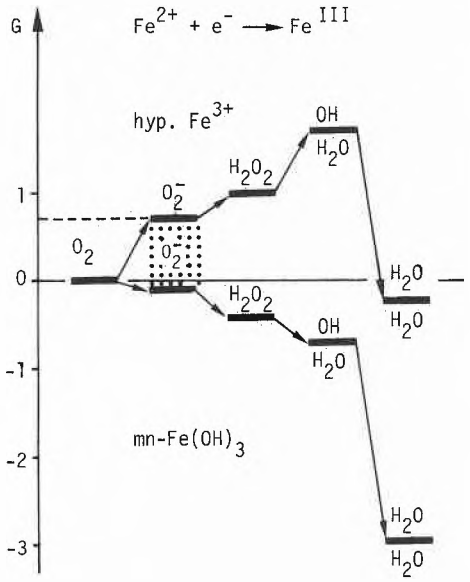

Fig. 10. Free energy profile of the oxygenation of hydrated ferrous ion. The instantaneous product of electron transfer is assumed to be either the hydrated ferric ion (upper part), or the mononuclear Fe(OH)$_3$ (lower part). Standard data are used including $E^o = +0.07$ V for the couple $O_2/O_2^{\ominus}$ at pH 7; overall stability constant β_3 of Fe(OH)$_3$: $\lg \beta_3 = 30$; G in the unit 96.5 kJ/mol.

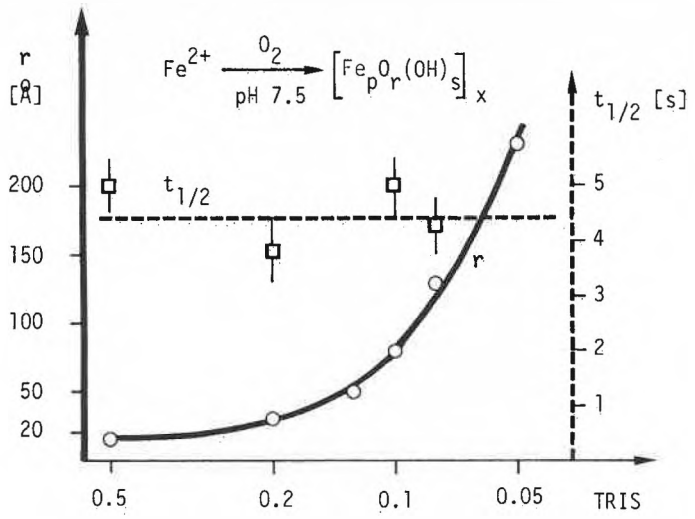

Fig. 11. Products of the oxygenation of 0.01 M iron(II) methanesulfonate in homogeneous solution (TRIS-buffer pH 7.5; room temperature). ○: The hydrodynamic radius r[Å] of dissolved iron(III) hydroxide particles. □: The half-time $t_{1/2}$ of the decay in 2M HCl. TRIS = $H_2NC(CH_2OH)_3$.

2.6. The Ferrous-Ferric Distribution

In biological systems, or rather in compartments such as cells and subcellular organelles, the ferrous-ferric distribution cannot be determined experimentally. It is all the more important to assess the factors involved in this distribution. With regard to the fundamental chemistry discussed above (Section 2.5), it is useful to consider two limiting cases:

a) The formation of polynuclears is inhibited, and there is a fast response in the distribution of $Fe^{2\oplus}$ and $Fe(OH)_i^{3-i}$ to changes of E_h.
b) The system is entirely thermodynamically controlled and α-FeO(OH) is the most stable solid phase.

It is seen from Fig. 12 that for a fixed total iron concentration the activity of $Fe^{2\oplus}$ depends very much on the kinetics of hydrolysis, or alternatively, that the $Fe^{2\oplus}$ activity depends very much on the type of hydrolysis products present at any instant. It has been suggested that $Fe^{2\oplus}$ could act as a messenger in intracellular iron regulation[51]. We do not know the relevant potential E_h in a cytoplasmic medium. However, if it were around + 0.2 V, the mononuclear $Fe(OH)_3$ could be an alternative to $Fe^{2\oplus}$ in the messenger role (cf. Sections 3.2 and 3.6).

3. Intracellular Iron Metabolism

By now much genetic information is available about the acquisition of microbial iron including uptake of iron and its regulation at the membrane level[32]. Chemically speaking, uptake involves either dissolution of iron hydroxides by siderophores («high affinity pathway») or reductive dissolution to ferrous ions («low affinity pathway»). We know neither the type nor the lifetime of the transient iron species occuring between membrane uptake and the insertion of iron at the physiological sites of action. It cannot be ignored that iron hydrolysis may not be such a prime aspect of intracellular chemistry in the microbial world as it is in the multicellular organisms to which we draw attention in this review.

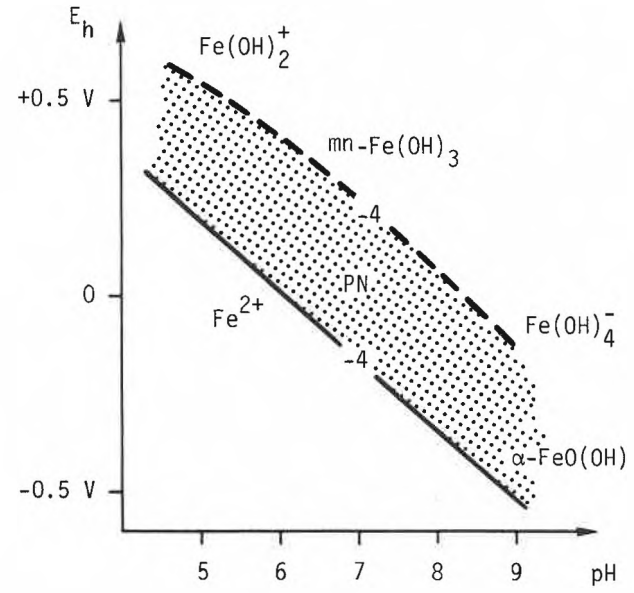

Fig. 12. The E_h/pH stability relationship between $Fe^{2\oplus}$ and ferric hydrolysis products at 25°C. Broken line: Equal concentrations, 10^{-4} M, of $Fe^{2\oplus}$ and the total of mononuclears $Fe(OH)_i^{3-i}$. Solid line: 10^{-4} M $Fe^{2\oplus}$ in equilibrium with α-FeO(OH). PN: Polynuclears with increasing (p; n̄) from the mononuclear to the α-FeO(OH) limit.

3.1. Phenomena and Interphenomena

There is a wealth of data on the proteins of iron transport and storage[52], in particular the molecular properties of proteins as well as their fate in cultured cells and laboratory animals. With regard to cells, most attention has been given to the iron metabolism of erythroid cells and hepatocytes. Considerable information was obtained when diferric transferrin was twin-labeled with ^{57}Fe and ^{125}I, and the intracellular distribution of both, iron and apotransferrin, was followed with powerful separation techniques. Some of the phenomena indicated in Fig. 13 can be inferred unambiguously from experiment.

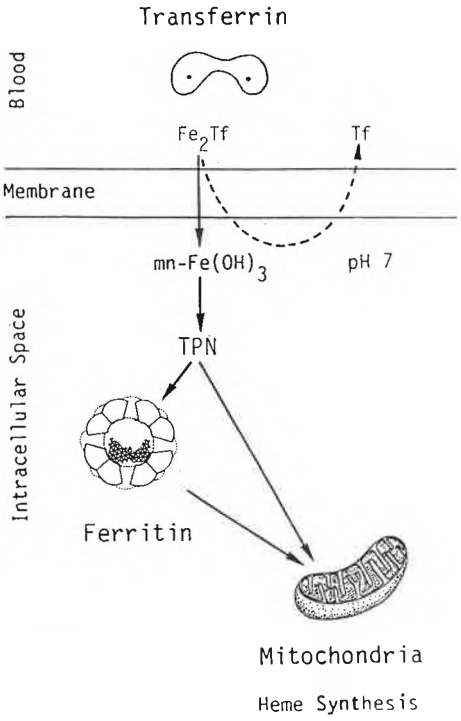

Fig. 13. Intracellular iron transport: Uptake of diferric transferrin, Fe_2Tf, is followed by the release of iron. The instantaneously formed species at pH 7.5 is mn-$Fe(OH)_3$. The transient polynuclears (TPN) are formed from mononuclears depending on the consumption rates by ferritin and mitochondria (Sections 3.5 and 3.6). The sizes of ferritin (diameter 0.012 μm) and mitochondria (length 1 μm) are not to scale.

Diferric transferrin, Fe_2Tf, is recognized and selectively bound by receptors at the cell surface. The iron is transferred from the protein into the intracellular space whereas the iron-free protein (apotransferrin) is recycled from the cell and released into circulation for re-utilization. Whether iron is released at the membrane level as a consequence of interactions with the receptor, or alternatively after internalization of the Fe_2Tf-receptor complex, can hardly ever be decided. There is experimental evidence for both mechanisms[52-54]. Labeled iron was found in the ferritin of reticulocytes some minutes after uptake from the extracellular Fe_2Tf, and its consumption by mitochondria for heme synthesis was observed to be the succeeding phenomenon[54].

The most important interphenomenon in the context of hydrolysis refers to the transient iron species which penetrate the protein shell of ferritin. The term *transit iron pool* was introduced to cover the sum of all intracellular species that are more readily available to chelators or react faster with reductants than either ferritin or heme iron[55]. We cannot trace either the intermediates that are involved when iron is used by the mitochondria for heme synthesis.

It is attractive, however, to combine results from in vitro studies with the phenomena identified in more holistic types of experiments in order to arrive at a consistent interpretation of the chemistry involved in the interphenomena.

3.2. Transient Iron Species in the Cytosol

It is well documented that the rate of iron uptake by erythroid cells is controlled by the number of transferrin receptors, which is of the order of 10^5 per cell[56]. The concept of an endocytotic cycle has found much support recently[52]. If diferric transferrin were internalized in rather acidic endosomes with pH as low as 5, the mechanism of release would be obvious because it has been verified in vitro[26].

In the present context it is irrelevant whether iron were transferred from Fe_2Tf directly to a neutral solution, or whether it proceeds via a slightly acidic region.

It was pointed out earlier[55] that the phenomenon of iron deposition in ferritin is not compatible with a thermodynamically controlled level of Fe^{III} species in the cytosol. Hydrolysis could be prevented either by powerful chelator on the one hand, or by reducing conditions, $E_h < +0.2$ V, on the other hand. However, transient species must be unstable with respect to the iron hydroxide phase as typified by ferritin.

The apparent paradox of localized iron hydroxide deposition in ferritin is removed at once if transient species have a much lower nuclearity than the ferritin core phase. Delayed hydrolysis in synthetic as well as in natural cytosols has been abundantly verified. It was shown that the cyclic polynuclears described in Section 2.3 persisted in neutral solutions containing high concentrations of groups such as –CONH–, ROH, $ROPO_3^{2\ominus}$ which in cytosols are provided by proteins, glycoproteins, carbohydrates, and organic phosphates. Moreover, polynuclears with low p were shown to be formed when $Fe^{2\oplus}$ was oxidized with oxygen in albumin solutions[57].

Recently, iron-containing low molecular weight fractions from rat reticulocyte cytosol were analyzed by modern HPLC methods[58]. These fractions had an apparent molecular weight of 5500, and contained glycine, cystine, citrate, and similar components but no specific «iron-binding proteins». It can be concluded that for these polynuclear cores p is well below 50, and that they are equivalent to those described in Sections 2.3 and 2.4. Therefore, it is justified to assume that they originated from mn-$Fe(OH)_3$. It is of interest that in this study, the conditions were chosen so as to inhibit heme synthesis and to uncouple oxidative phosphorylation. Hence, the intracellular concentration of transient iron species had been artificially raised with respect to the normal state.

3.3. Iron Deposition in Ferritin

X-ray and electron diffraction evidence have led to the repeated conclusion that the mineral core of ferritin has a structure resembling that of synthetic ferrihydrite. Recently, it was emphasized that the structure depends markedly on the origin of the specimen. Whereas human ferritin (spleen) and hemosiderin particles were found to be single-domain crystals with a ferrihydrite structure, ferritin from limpets contained rather amorphous iron hydroxide[59]. The comparison with ferrihydrite is to some extent misleading since natural ferrihydrite differs from the synthetic preparation, and neither material is structurally as well defined as the FeO(OH) phases mentioned in Section 1.1.

The present author believes that ferritin cores may consist of rather mobile low-nuclear species, or of fairly tight aggregates of such polynuclears, or even some crystallites. The experimental proof of this view is pending. The key experiment is the reproduction of ferritin cores in the same way that it occurs in vivo.

It is easy to incubate apoferritin with ferrous salts in the presence of molecular oxygen or other oxidants. Fe^{II} ions and O_2 molecules can penetrate the protein shell to form iron(III) hydroxide. It is doubtful whether biological pathways of deposition involve Fenton-type reactions between $Fe^{2\oplus}$ and O_2 with a total of some 1000 to 2000 electrons transferred from ferrous ions to oxidant molecules or radicals, respectively.

Ferric salts are not useful educts because they hydrolyze during the mixing procedure in neutral solution, and the polynuclears so formed are unable to penetrate the protein shell.

It was observed recently that even cyclic polynuclears with p = 6 (Section 2.4) are too large for shell penetration[60]. It has been concluded that the ideal source of iron is mononuclear $Fe(OH)_3$. In this case there is no barrier to nucleation because the substitution reaction (20) and subsequent growth steps are very fast. Once formed, the primary polynuclears would be expected to aggregate. In this context, the most valuable physical data are Mössbauer spectra[61] which indicate that the iron(III) in the ferritin cage is mobile above some «melting temperature» probably related to the melting of ice. This result supports the idea of aggregated primary polynuclears, similar to those identified in synthetic solutions, emerging from mn-$Fe(OH)_3$ (Section 2).

Clearly, it is very desirable to assess the possible lifetimes of transient species which depend upon the interplay between the cellular iron uptake, the uptake of transient species by ferritin, and the iron consumption by mitochondria.

3.4. Iron Mobilization from Ferritin

This is an intriguing problem because mobilization seems to oppose the storage function in a non-equilibrium system where the iron flux is a vector from ferric transferrin to heme. However, it is customary to separate the questions related to the network of intracellular reactions (Section 3.6) from the questions related to the chemical dissolution of the ferritin core.

As pointed out by *Crichton*[52], mobilization by chelating ligands can be ruled out because it is far to slow. The alternative is reductive dissolution. The kinetic characteristics of iron release by dithionite, thioglycolate, and dehydroriboflavin-5-phosphate ($FMNH_2$) have been studied and found to differ widely[62] due to specific surface interactions of $SO_3^{2\ominus}$ (from $S_2O_4^{2\ominus}$), $^{\ominus}O_2CCH_2SH$, and $FMNH^{\ominus}$ with iron(III) sites. In the present context, it is of prime importance that the reactions occur at the iron hydroxide surface, which means, within the ferritin core. This requirement rules out any «reflux» of small core fragments to the extraprotein space which might have been expected to be the rate-determining step in reduction at the interface protein/cytosolic solution.

Incidentally, this conclusion supports the concept of a non-equilibrium situation between cytosolic iron species and the ferritin core phase.

With regard to the time scale involved, it is obvious from the reduction study[62] that reductive mobilization is the realistic pathway. This in turn draws attention to the mitochondrial consumption of iron(III) species for heme synthesis.

3.5. Mitochondrial Iron Consumption

It is very difficult to imagine how the intracellular donor of iron to the mitochondria could be unambiguously identified. However, it is challenging to compare well-defined donors in experiments with isolated mitochondria. The methodology required has been developed and sucessfully applied by *Romslo* et al.[63] who showed that ferritin iron can be reductively mobilized by electrons of the respiratory chain of isolated mitochondria, mediated by exogenous FMN. This iron is then incorporated into deuterioporphyrin IX. This leaves unanswered the question of whether ferritin is an obligatory intermediate in iron utilization for heme synthesis, or whether it is merely a sink for excess iron. As an alternative to ferritin, transit pool species, by definition all species other than ferritin, could be an iron source for heme synthesis.

Recently, a comparative study of iron sources including ferritin and models of transit pool species was carried out[57]. Sorbitol, gluconate, and bovine serum albumin were used as scavengers for polynuclears with restricted size. Ferritin was shown to supply iron readily for heme synthesis if the ferritin iron was reductively mobilized by the mitochondrial respiratory chain with succinate as substrate and FMN as mediator. No FMN was required when polynuclear iron(III) complexes were reacted to form deuterioporphyrin. The kinetic data in Table 4 are most revealing with regard to the polynuclear iron(III) sources.

Although the nuclearity changes by a factor of at least two orders of magnitude, the rates of deuterioheme formation do not differ much. Rates of acid decomposition of polynuclears, and of dissolution by chelators, are by no means proportional to the nuclearity p, and they differ by a factor of 10000 between the hexanuclear and the polymaltose protected polynuclear (Table 4). The protein shell of ferritin apparently does not delay iron liberation any more than does the polymaltose preparation. Surprisingly, ferritin and transit pool iron species are largely equivalent sources for mitochondrial heme synthesis. This suggests that the protein shell may possibly be broken up by interaction with the mitochondrial membrane.

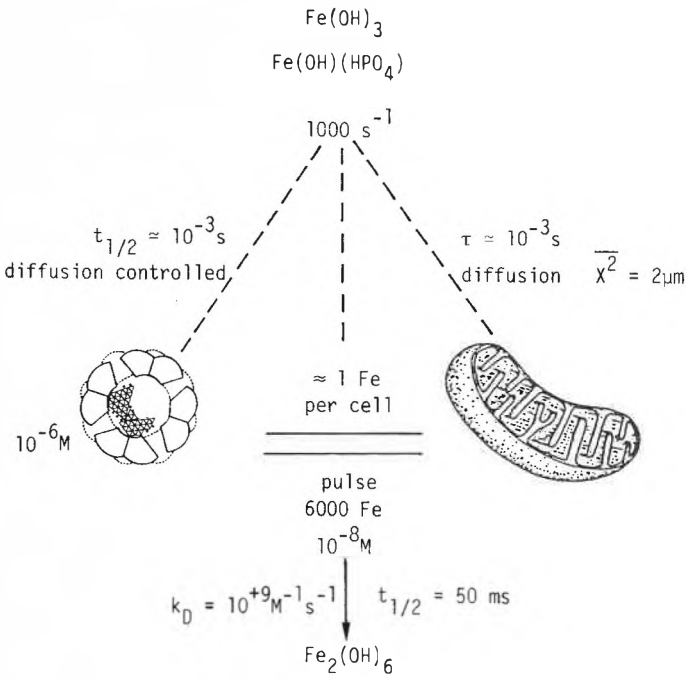

Fig. 14. Competitive processes involving mononuclear transient species mn-$Fe(OH)_3$ or $Fe(OH)(HPO_4)$: iron deposition in ferritin, mitochondrial consumption, and self-reaction. $\tau = \bar{X}^2/2D$; $D = 2 \cdot 10^{-5} cm^2 s^{-1}$. The numerical examples illustrate that delocalized deposition of iron hydroxide can be avoided kinetically.

The very stable $[Fe(EDTA)]^{\ominus}$ and Ferrioxamin B are not utilized for heme synthesis. This is an important observation in the context of cytosolic iron binding. Very strong chelators which prevent iron hydrolysis would also rule out ferritin core formation, and in addition, they would inhibit the supply of iron to mitochondria.

3.6. Synopsis: How Ferritin is Filled

Intracellular iron metabolism includes a variety of uptake and excretion processes[52,64] which we do not consider here since iron donation by transferrin is the major pathway of cellular iron uptake. This pathway is unique in that mononuclear hydroxo species are delivered to the cytoplasma. Some transit pool iron is used for the synthesis of iron-containing enzymes, but this does not affect the evaluation of the fluxes to ferritin, and further to the mitochondria.

The requirement for iron and its utilization for heme synthesis is particularly noticeable in erythropoesis, the production of red cells from the bone marrow. The first stage (amplification) involves a series of four to six cell divisions. The lifespan of each generation is around 20–24 h. From morphological and analytical data the following average quantities can be estimated[65]:

Iron uptake from transferrin:	10^{-15} mol per cell per 20 h
Flux of iron into the cell:	8000 atoms Fe per second
Volume of the cell:	10^{-12} to 10^{-13} liter (L)
Increment of iron concentration:	10^{-3} to 10^{-2} mol/L per 20 h 10^{-8} to 10^{-7} mol/L per second

To our knowledge there are no cells requiring higher fluxes of iron than the cells of the erythrocytic series. Consequently, the following conclusions should be generally valid. The numerical values of the entities in Fig. 14 are based on a flux of 1000 atoms Fe per second. We estimate:

a) The average time τ between collisions of a mononuclear iron species with a mitochondrion. Assuming that the distance from an iron atom released to a mitochondrion is 2 μm, and that the latter is at rest relative to the iron species, the value $\tau = 10^{-3}$s is estimated from *Einsteins* equation.

b) The half-time of a second order reaction of mn-$Fe(OH)_3$ with an apoferritin or (partly filled) ferritin molecule. The ferritin concentration is remarkably high, about 10^{-6} mol/L. The mn-$Fe(OH)_3$ is equivalent in size to hydrated $Fe^{2\oplus}$ but more versatile in the

Table 4. Mitochondrial heme synthesis from different sources of iron. Relative rates of deuterioheme formation in isolated yeast mitochondria; total iron was around 0.5 mM; pH 7.4; 37 °C. Data from *Funk* [57].

Iron(III) source	Relative rate of deuterioheme formation	Decay of iron complex in 2M HCl $t_{1/2}$ [s]
$[Fe(EDTA)]^{\ominus}$	0	
[Fe(DFB)]	0	
$[Fe(tir)_3]^{9\ominus}$	0	
ferritin (2000)	1	
$[Fe_6(OH)_{12}(sor)_6]$	3.3	0.11
+ bovine serum albumin	1.3	
PN/sorbitol[a] gluconate	2.9	0.34
$[FeO(OH)]_{p \approx 1000}$ polymaltose[b]	0.4	330

[a] Prepared from highly alkaline sorbitol/gluconate solution.
[b] Commercial preparation.

interactions with the protein. That's why it is expected to penetrate the protein shell even more easily than $Fe^{2\oplus}$. It must be postulated that the «reaction» with ferritin is diffusion-controlled. This implies a second order rate constant k_D of the order $10^9 M^{-1}s^{-1}$, and the half-time $t_{1/2}$ of the pseudo-first order reaction is about 1 ms.

Clearly, the rates of removal of transient mn-$Fe(OH)_3$, both by ferritin and by mitochondria are comparable with the rate of iron release from transferrin. Consequently, the steady state concentration of transient species is very low indeed. Under these conditions, the rate of formation of polynuclears is very slow compared to the rate of their removal.

A pulse of 6000 mononuclears $Fe(OH)_3$, 10^{-8} mol/L, would form dinuclears within 50 ms; this half-time is much longer than that for the uptake of mn-$Fe(OH)_3$ by ferritin.

We arrive at the conclusion that the ferritin core space is acting as a cage for mn-$Fe(OH)_3$. The concentration of mn-$Fe(OH)_3$ increases very steeply with p, reaching values of around 0.1 M for p = 15, which leads to half-times of dimerization of around 50 ps. Any binding for $Fe(OH)_3$ at the inner surface of the protein would greatly enhance the formation of the ferritin core.

4. Perspectives

In organisms, many stages in pathways of iron hydrolysis and the products involved cannot be elucidated experimentally. This limitation particularly concerns the formation and consumption of transient species in cells and in their subcompartments. Any experiment, designed to isolate or identify these species involves a prohibitive perturbation of the system. In such instances the only way to bridge the gap between those phenomena that are amenable to experiment, is to take into consideration all the possible molecular events involved. In this context, the design of experiments which simulate at least some aspects of the biological situation is becoming increasingly important.

Biological pathways of hydrolysis tend to circumvent conditions which favour crystalline phases. On the other hand, it is feasible that the quality of ferritin cores may be an important physiological indicator. Hence, it is important to establish realistic interactions which could induce the «ageing» of ferritin cores, i.e. processes that increase the cristallinity of the core and lower the radio P/Fe. With regard to the internal iron cycle, there is an enormous gap in our understanding of the pathways by which iron emerges from the destruction of red cells.

Acknowledgements: I am very much indebted to Christian Anner, Isidor Erni, Felix Funk, Martin Glaus, Dieter Hametner, Urs von Guten, Jan Jiskra, Rainer Kündig, Werner Künzi, Eleonore Mathier-Landa, Nik Oswald, Hans W. Rich, Bruno Rüttimann, Bernhard Schwyn, Frank van Steenwijk for their participation in these studies. Research was supported by Kredite für Unterricht und Forschung, ETHZ; Laboratorien Hausmann AG, St. Gallen; Swiss National Science Foundation (Project No. 2.382-0.84); Robert Gnehm Fonds. I thank Dr. Rochelle Cornell for the assistance in the preparation of the manuscript.

Received: July 20, 1987 [FR 46]

[1] W. Schneider, B. Schwyn, in W. Stumm (Ed.): *Aquatic Surface Chemistry*, Wiley-Interscience, New York (1987), p. 167.
[2] W. Schneider, *Comments Inorg. Chem. 3* (1984) 205.
[3] K.H. Wedepohl: *Handbook of Geochemistry*, Vol. *II-3*, Springer, Berlin (1969), p. 26-D-1.
[4] T.D. Waite, F.M.M. Morel, *J. Colloid Interface Sci. 102* (1984) 121; R.G. Zepp, N.L. Wolfe, in W. Stumm, *loc. cit.* [1], p. 443.
[5] W. Stumm, P. Baccini, in A. Lerman (Ed.): *Lakes – Chemistry, Geology, Physics*, Springer, Berlin (1978), p. 65.
[6] B.F. Jones, C.J. Bowser, in A. Lerman, *loc. cit.* [5], p. 179.
[7] R.M. Cornell, R. Giovanoli, *Clays Clay Miner. 33* (1985) 424, and references quoted therein.
[8] U. Schwertmann, R.M. Taylor, in J.B. Dixon, S.B. Weed (Ed.): *Minerals in Soil Environments*, Soil Sci. Soc. of America, Madison WI (1977), p. 145.
[9] V.F. Fairbanks, E. Butler, in W.J. Williams, E. Butler, A.J. Erslev, M.A. Lichtman (Ed.): *Hematology*, McGraw-Hill, New York (1983), p. 300.
[10] C. Kies, L. McEndree, in C. Kies (Ed.): «Nutritional Bioavailability of Iron», *ACS Symp. Ser. 203* (1982) 183.
[11] W. Schneider, *Arzneim. Forsch./Drug. Res. 37(1), 1a* (1987) 92.
[12] W. Forth, *Naturwissenschaften 74* (1987) 175.
[13] W. Schneider. W. Forth, *Arzneim. Forsch./Drug. Res. 37(1), 1a* (1987) 89.
[14] R.A. Cooper, J.H. Jandl, in W.J. Williams et al., *loc. cit.* [9], p. 377.
[15] M. Bessis, L.S. Lessin, E. Butler, in W.J. Williams et al., *loc. cit.* [9], p. 257.
[16] A. Erslev, in M.J. Williams et al., *loc. cit.* [9], p. 365.
[17] E.R. Hughes, in H. Sigel (Ed.): *Metal Ions in Biological Systems*, Vol. *7*, Marcel Dekker, New York (1978), p. 301.
[18] P. Harrison, in E.C. Theil, G.L. Eichhorn, L.G. Marzilli (Ed.): *Advances in Inorganic Biochemistry*, Vol. *5*, Elsevier, Amsterdam (1983), p. 39.
[19] M. Heusterspreute, R.B. Crichton, *FEBS Lett. 129* (1981) 322.
[20] E.C. Theil, in E.C. Theil et al., *loc. cit.* [18], p. 1.
[21] A. Jacobs, in A. Jacobs, M. Worwood (Ed.): *Iron in Biochemistry and Medicine*, Vol. *II*, Academic Press, New York (1980), p. 427.
[22] C.A. Finch, in W.J. Williams et al., *loc. cit.* [9], p. 713.
[23] D.J. Weatherall, in W.J. Williams et al., *loc. cit.* [9], p. 493.
[24] W. Schneider, in E.D. Goldberg (Ed.): *The Nature of Seawater*, (Dahlem Workshop Report), Dahlem Konferenzen, Berlin (1975), p. 375.
[25] P. Schindler, W. Michaelis, N. Feitknecht, *Helv. Chim. Acta 46* (1963) 444.
[26] P. Aisen, I. Listowsky, *Annu. Rev. Biochem. 49* (1980) 357.
[27] J.M. Berg, R.H. Holm, in T.G. Spiro: *Iron-Sulfur Proteins*, Wiley, New York (1982), p. 33.
[28] J.H. Brock, in P. Harrison (Ed.): *Metal Proteins with Non-redox Roles*, Verlag Chemie, Weinheim (1985), p. 183.
[29] P.W. Schindler, W. Stumm, in W. Stumm, *loc. cit.* [1], p. 83.
[30] W. Stumm, R. Kummert, L. Sigg, *Croat. Chem. Acta 53* (1980) 291.
[31] This is easily deduced from stability data. D.D. Perrin: *Stability Constants of Metal Ion Complexes, Part B: Organic Ligands*, Pergamon, Oxford (1979); E. Högfeldt: *ibid., Part A: Inorganic Ligands* (1982).
[32] J.B. Neilands, K. Konopka, B. Schwyn, M. Coy, R.T. Francis, B.H. Paw, A. Bagg, in F. van der Helm, J.B. Neilands, G. Winkelmann: *Ion Transport in Microbes, Plants, and Animals*, VCH Verlagsgesellschaft, Weinheim (1987).
[33] G. Biedermann, P.W. Schindler, *Acta Chem. Scand. 11* (1957) 731.
[34] W. Feitknecht, W. Michaelis, *Helv. Chim. Acta 45* (1962) 212.
[35] G. Biedermann, J.T. Chow, *Acta Chem. Scand. 20* (1966) 1376.
[36] P.R. Danesi, R. Chiarizia, G. Scibona, P. Riccardi, *Inorg. Chem. 12* (1973) 2089.
[37] H.B. Gray, *Recent Chem. Prog. 29* (1968) 163; H.J. Schugar, G.R. Rossman, H.B. Gray, *J. Am. Chem. Soc. 91* (1969) 4564.
[38] G. Anderegg, *Helv. Chim. Acta 45* (1962) 1643.
[39] E.B. Fleischer, T.S. Scrivastara, *J. Am. Chem. Soc. 91* (1969) 2403.
[40] J. Lewis, B.N. Figgis, A. Earnshaw, *J. Chem. Soc. A* (1966) 1656.
[41] B. Lutz, H. Wendt, *Ber. Bunsenges. Phys. Chem. 74* (1970) 372.
[42] S.J. Lippard, *Chem. Br. 22* (1986) 222.
[43] R.G. Wilkins, P.C. Harrington, in E.C. Theil et al., *loc. cit.* [18], p. 51.
[44] E. Mathier, Dissertation Nr. 8154, ETH Zürich (1986).
[45] F. van Steenwijk, D. Hametner, W. Schneider, *Proc. Workshop Chem. Appl. Mössbauer Spectrosc., Seeheim FRG* (1978) 17.
[46] W. Schneider, I. Erni, D. Hametner, B. Magyar, F. van Steenwijk, *Inorg. Chim. Acta, Bioinorg. Chem.*, in press.
[47] H.W. Rich, Dissertation Nr. 8231, ETH Zürich (1987).
[48] W. Sung, J.J. Morgan, *Environ. Sci. Technol. 14* (1980) 561; W. Stumm, J.J. Morgan: *Aquatic Chemistry*, Wiley, New York (1981), p. 238, 331, 418.
[49] B.J. Berne, R. Pecora: *Dynamic Light Scattering*, Wiley, New York (1976).
[50] U. von Gunten, ETH Zürich, unpublished work.
[51] R.J.P. Williams, *FEBS Lett. 140* (1982) 3.
[52] Recent comprehensive review: R.R. Crichton, M. Charloteaux-Wauters, *Eur. J. Biochem. 164* (1987) 485.
[53] C. van der Heul, A. Veldlman, M.J. Kroos, H.G. van Eijk, *Int. J. Biochem. 16* (1984) 383.
[54] M.T. Nunez, J. Glass, *J. Biol. Chem. 260* (1985) 14707.
[55] W. Schneider, I. Erni, in P. Saltman, J. Hegenauer (Ed.): *The Biochemistry and Physiology of Iron*, Elsevier, New York (1982), p. 121.
[56] B.J. Iacopetta, E.H. Morgan, G.C.T. Yeoh, *Biochim. Biophys. Acta 687* (1982) 204.
[57] F. Funk, C. Lecrenier, E. Lesuisse, R.R. Crichton, W. Schneider, *Eur. J. Biochem. 157* (1986) 303.
[58] D.L. Bakkeren, C.M.H. De Jeu-Jaspars, C. van der Heul, H.G. van Eijk, *Int. J. Biochem. 17* (1985) 925.
[59] S. Mann, J.V. Bannister, R.J.P. Williams, *J. Mol. Biol. 188* (1986) 225.
[60] I. Erni, R. Kündig, W. Schneider, communication to the European Iron Club Meeting, Pavia (1987).
[61] S. Ofer, E.R. Bauminger, S.G. Cohen, I. Nowik, in I. Urushizaki, P. Aisen, I. Listowsky, J.W. Drysdale (Ed.): *Structure and Function of Iron Storage and Transport Proteins*, Elsevier, Amsterdam (1983), p. 59.
[62] F. Funk, J.P. Lenders, R.R. Crichton, W. Schneider, *Eur. J. Biochem. 152* (1985) 167.
[63] I. Romslo, in A. Jacobs et al., *loc. cit.* [21], p. 325.
[64] B.R. Bacon, A.S. Tavill, *Semin. Liver Diseases 4* (1984) 181.
[65] M. Bessis: *Blood Smears Reinterpreted*, Springer, Berlin (1977), p. 25.